

DEPENDENCE OF X-RAY GENERATION OF INTERFACE TRAPS ON
GATE METAL INDUCED INTERFACIAL STRESS IN MOS STRUCTURES

Viktor Zekeriya and T-P. Ma
Yale University, Department of Electrical Engineering
New Haven, Connecticut 06520

ABSTRACT

In a series of experiments, we deliberately altered the interfacial stress distribution in MOS structures by varying the mechanical properties of the gate Al films. Subsequently, we found that the generation of interface traps resulting from exposure to X-ray was strongly correlated to this stress distribution. For a given oxide process and radiation dose, a universal curve could be established, which relates the density of radiation-induced interface traps to the interfacial stress distribution. An explanation based on the strained bond model will be proposed, which incorporates the effect of the gate-induced stress distribution on the oxide bond strain gradient near the SiO_2/Si interface.

INTRODUCTION

It is a well recognized fact that generation of interface traps in MOS devices could take place upon exposure to ionizing radiation. While the generation mechanisms are not yet completely understood, most models that have been proposed involve breaking of bonding sites containing H [1-3], OH [3-5], or strained bonds [5-10] in SiO_2 or at the SiO_2/Si interface.

A strained SiO_2 region near the SiO_2/Si interface has been shown to exist [5,6], and the authors proposed that the radiation induced interface trap density depends on the bond strain gradient in the oxide [3]. The possibility that mechanical stress might affect the MOS radiation sensitivity through its influence on the strained bonds was first suggested by Chin and Ma [11], who observed strong dependence of the radiation-induced interface traps on the gate linewidth, which they attributed to the variations in the gate-induced interfacial stress distribution.

In recent publications [13,14], we reported that both the interfacial stress distribution and the radiation induced interface trap density systematically change with gate Al thickness [13] and time lapse between PMA and irradiation [14] in $\text{Al}/\text{SiO}_2/\text{Si}$ devices, and established strong correlation between the two.

In this paper, we describe several new experiments in addition to the previous ones, and the results further confirm that the interfacial stress distribution is an important factor which affects the generation of interface traps in MOS devices subjected to ionizing radiation. A model will be introduced which describes qualitatively how the externally introduced mechanical stress could affect the overall bond strain distribution, and its resultant effect on the radiation sensitivity in a MOS structure.

EXPERIMENTAL PROCEDURES

The samples were made on p-type Si (100) wafers of 1 Ω -cm resistivity and 9 mil thickness. The oxides were grown in dry O_2 at 1040 C to a thickness of approximately 500Å, followed by in-situ annealing in

N_2 at the growth temperature for 30 minutes. After the oxidation, Al films of thickness ranging from 500Å to 13000Å were thermally evaporated from a Ta boat on to the oxide surface. Most of the samples studied had circular gates of 25 mils in diameter. Some of the wafers were completely covered with Al to be used in curvature measurements. For the gate thickness dependence experiment, a multiple evaporation procedure was used to deposit four different thicknesses of Al on different areas of the same wafer. The back side of the wafers were coated with a thin (typically 150Å) layer of Al to serve as the contact. Following this, some of the samples were post-metal-annealed (PMA) while the rest were not, in order to compare the difference in their interfacial stresses as well as radiation sensitivities. The radiation source was an X-ray beam generated from either a Cr or W target bombarded by 35 keV electrons. For the gate thickness dependence experiment, the irradiation was from the back side of the wafer, so that variations in the penetrated X-ray intensity due to absorption by different gate Al thicknesses could be avoided, although irradiation from the front side with thick (1-4 mils) Al filters was also performed, yielding qualitatively similar results. The dosages in this paper correspond to those absorbed in the oxide estimated by taking into account the absorption by the thick silicon wafer. No bias was applied to the devices, which were left floating during irradiation.

The density and energy distribution of the interface traps were calculated from the high frequency and quasi-static C-V curves measured before and after irradiation. As a result of the irradiation, a 'characteristic peak' [8,9,15] developed at around 0.2 eV above midgap, the magnitude of which was used to characterize the radiation sensitivity of the devices, as was done previously [13-15].

All data presented here were obtained from at least two sets of wafers processed at different times, and for each point, 6 to 10 devices were measured to assure reproducibility and uniformity.

The stress distribution was determined by measuring the curvature of the wafers using a laser beam reflection technique [12,13], and then converting the curvature values to stresses using a bimetallic beam theory [16], which was modified to include more than two layers [17]. A good agreement was found between the calculated and measured curvature values.

As will be further elaborated in the discussion, among the various stress components in the MOS structure, two were found to be possible candidates in affecting the radiation sensitivity of the devices: The silicon surface stress σ_{Si} (on the silicon side of the interface) and the oxide stress gradient $\nabla \sigma_{\text{SiO}_2}$ (defined as the change in the oxide stress per unit oxide thickness). Once the curvature is known, these values can be calculated from:

$$\sigma_{si,1} = \frac{E_{si}}{(1-\nu)_{si}} k h_{si} \quad (1)$$

$$\nabla \sigma_{SiO_2} = \frac{E_{SiO_2}}{(1-\nu)_{SiO_2}} k \quad (2)$$

where E_{si} and E_{SiO_2} are the Young's moduli of the silicon and the oxide, k is the curvature, ν is the Poisson's ratio, d_{ox} is the oxide thickness and h_{si} is the distance from the neutral axis, which can be taken as $\frac{2}{3} d_{si}$ (silicon thickness) within the range of studied samples [15]. $\frac{E_{si}}{(1-\nu)_{si}}$ and $\frac{E_{SiO_2}}{(1-\nu)_{SiO_2}}$ were taken as 1.805×10^{12} dynes/cm² and 8.64×10^{11} dynes/cm², respectively [18,19].

Theoretically the curvature k is related to the other parameters approximately by [17]

$$K = 6 \frac{E_{Al} d_{Al} \Delta T_{Al} (\alpha_{Al} - \alpha_{Si}) - E_{ox} d_{ox} (\alpha_{Si} - \alpha_{ox}) \Delta T_{ox}}{E_{si} d_{si}^2} \quad (3)$$

where d_{Al} is the Al film thickness, ΔT_{Al} is the temperature difference between PMA and room temperature, α 's are the thermal expansion coefficients, and ΔT_{ox} is the temperature difference between oxidation and room temperature.

Experimentally, it has been found that the curvature after PMA is somewhat lower than the theoretical value, due to the stress relaxation effect of the Al film.

RESULTS

Gate-Al Thickness Dependence: Figure 1 shows the quasi-static C-V curves for three samples with different Al thicknesses after being irradiated to a dose of about 3 Mrads (Si). The irradiation was done 20 hours after the samples were post-metal-annealed. The pre-irradiation curve is essentially the same for all devices, and is represented by the dotted curve. The voltage axes have been shifted so that they all line up in the accumulation region for easy comparison. Figure 2 shows the energy distribution of the radiation-induced interface trap density ΔN_{it} for the above devices. As usual [8,9,13-15], a 'characteristic peak' develops at about 0.2 eV above midgap, the magnitude of which strongly depends on the gate Al thickness.

Figure 3 shows the magnitude of this radiation-induced peak as a function of the Al gate thickness for devices both with and without PMA. It is apparent that the curve for PMA treated devices shows a monotonic decrease as the Al thickness increases, and tends to gradually saturate beyond about 10000Å. The no PMA curve shows some initial drop, after which it seems to scatter about a saturation value. The difference between annealed and not annealed devices tends to decrease as the gate Al thickness is reduced.

In parallel with the radiation experiments, we performed curvature measurements to determine the interfacial stress distribution of our devices as a function of the various process parameters. The results are shown in Fig. 4, where we plotted the

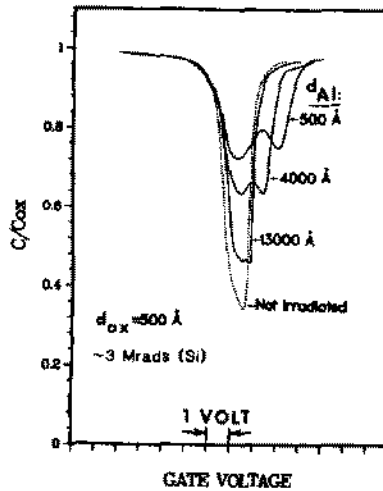


Fig. 1. Quasi-static C-V curves for three samples with different gate Al thicknesses that were irradiated 20 hours after PMA. The curves have been shifted along the voltage axis to line up in accumulation.

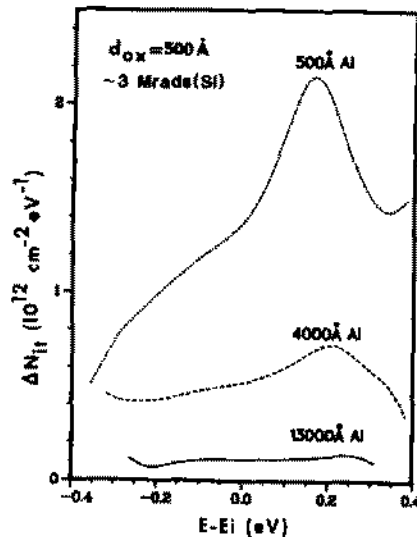


Fig. 2. Energy distribution of the radiation-induced interface trap density ΔN_{it} for the three samples shown in Fig. 1.

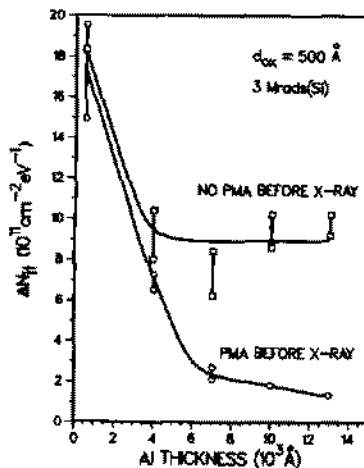


Fig. 3. Dependence of the radiation-induced interface trap peak density on gate Al thickness for both annealed and not annealed devices.

oxide stress gradient and the Si surface stress (which are related by a multiplicative constant as can be seen from (1) and (2)) as a function of the gate Al thickness. Due to a stress relaxation effect to be discussed in the next section, we include three different curves for the PMA samples based on the different time lapse after PMA. For all conditions depicted in Fig. 4, the oxide stress gradient and the silicon surface stress change monotonically with Al thickness, and the extent of the change depends strongly on whether the sample received PMA and the time lapse after PMA. Comparing Figs. 3 and 4, there

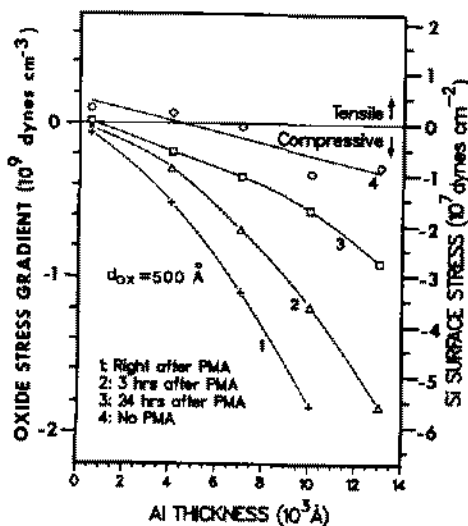


Figure 4 Dependence of the oxide stress gradient and Si surface stress on gate Al thickness for four different conditions as specified.

is evidently a correlation between ΔN_{it} and the oxide stress gradient (or the Si surface stress).

Effect of Stress Relaxation: As mentioned earlier, the interfacial stress distribution was found to change systematically with time lapse after PMA. Figures 5 and 5 clearly show this stress relaxation effect. As can be seen from Fig. 5, the time constant for the relaxation process is on the order of a few hours, and after 24 hours, the stress approaches its saturation value for all four gate Al thicknesses. To study possible correlations of this effect with the device radiation sensitivity, we divided the samples into three lots for each gate Al thickness and irradiated the first lot immediately after PMA, the second lot 3 hours after PMA, and the third 24 hours after PMA. The irradiation time was 15 minutes for all samples. Figure 6 shows the radiation-induced interface trap peak density as a function of the time lapse between PMA and irradiation for three different Al thicknesses. Two distinct features are apparent: The generated trap density depends on the Al thickness, as was shown in context with another experiment in the previous section, and for a given thickness, it is a function of the time lapse between annealing and irradiation. It should be noted that no such dependence was observed for the trap densities of pre-irradiation devices.

One cannot help but notice the striking similarity between Figs. 5 and 6 in their time dependence. To examine this possible correlation more closely, in Fig. 7 we plotted ΔN_{it} as a function of the oxide stress gradient and the Si surface stress, using the data in Figs. 4-6. It is interesting to note that although the data points are taken from several devices with a wide range of Al thicknesses and time lapses after PMA, the resulting curve is pretty smooth and shows very little scattering. The existence of such a 'universal curve' suggests that the interface stress distribution may be a fundamental parameter that affects the generation of interface traps. It should be noted that different oxidation processes and radiation doses will give rise to different 'universal curves'.

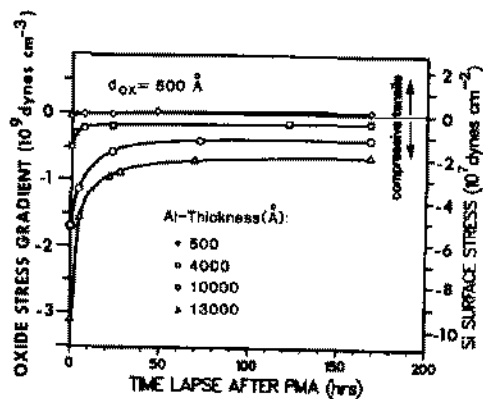


Figure 5 Dependence of oxide stress gradient and Si surface stress on time lapse between PMA and irradiation for different gate Al thicknesses.

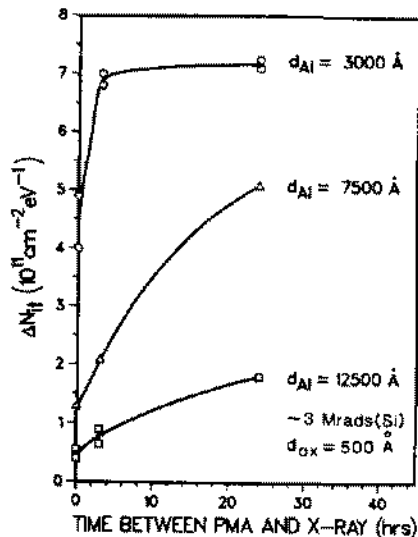


Figure 6 Dependence of radiation-induced interface trap generation on time lapse between PMA and irradiation for three gate Al thicknesses.

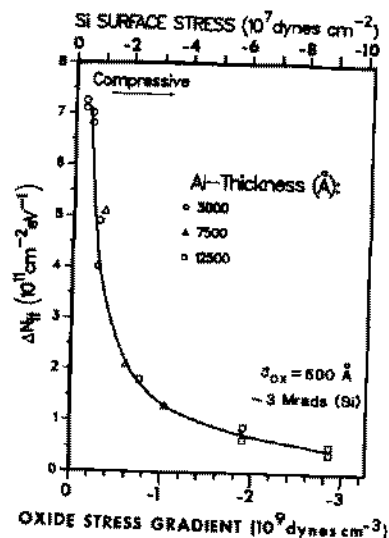


Figure 7 Dependence of radiation-induced interface trap generation on oxide stress gradient and Si surface stress from the data shown in Figs. 4-6.

Edge Effect: It has been shown both theoretically [20] and experimentally [21,22] that a film edge on a continuous substrate will affect its stress distribution near the discontinuity in such a way that the stress due to the discontinuous film will be largest at the edge and will fall down as a function of distance from this edge. To check the effect of this spatially varying stress on the radiation sensitivity, we performed the following experiment:

Large square capacitors, 93 mils on one side, were defined photolithographically after metallization, and the devices were irradiated three hours after PMA. If the radiation sensitivity really depends on the stress distribution, one would expect a spatial distribution of ΔN_{it} under the gate so that the density near the edge should be different from that near the center. To investigate this spatial variation, we used a second mask shown, in Fig. 8. After the completion of irradiation, this mask was aligned with the original square pad and a set of MOS capacitors with various distances from the edge of the Al pad were defined. The baking of photoresist in the photolithography step was done at no more than 50 C to minimize annealing effects. Figure 9 shows the quasi-static C-V curves for devices with various distances from the edge, where curve 1 corresponds to the device closest to the edge and curve 4 closest to the center. As one can see, there is indeed a systematic increase in the interface trap density as the probed area approaches the center. Unirradiated devices were also measured and showed no spatial variation, as expected. This is shown by curve (0) together with a high frequency C-V curve for reference. Figure 10 shows the dependence of the interface trap generation on the linear distance from the edge for two different Al thicknesses. As usual, the thickness dependence can be seen in addition to a strong spatial variation of ΔN_{it} . The trap generation is smallest right at the edge, increases as one moves away from the edge and begins to saturate between 40 and 50 mils from the edge.

These results again strongly support a close relationship between interfacial stress and trap generation. The faster saturation of the curve for 8000Å of Al can be understood on the basis of Fig. 7, which implies a nonlinear relation between trap generation and stress. A similar effect was observed for the midgap voltage shift and will be reported in more detail in a subsequent publication.

Growth of ΔN_{it} with Time* after Irradiation

We observed a time dependent increase in the interface trap density at room temperature after the irradiation was completed. Virtually all the devices which were measured showed the same phenomenon. Figure 11 shows this time dependent behavior for several samples with 500Å oxide and various gate Al thicknesses. The samples were irradiated 3 hours after PMA, and left at room temperature with no voltage bias. We should note here that a time dependent evolution of interface traps has been reported previously [23,24], but in those cases a voltage bias was applied to the devices throughout the sampling period.

In addition to the long time constant involved in the process, Fig. 11 indicates that samples with thinner Al gate have a faster rate of increase. The implications of these results will be discussed in the next section.

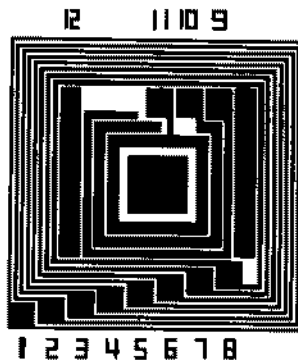


Fig. 8 Second level mask used to determine the spatial variation of the radiation-induced interface trap density under the Al pad. The outer dimensions are 92.8 x 92.8 mils.

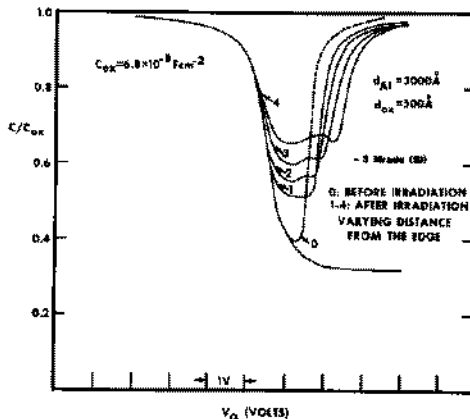


Fig. 9 Quasi-static C-V curves for devices shown in Fig. 8 with the following distances from the edge: (1) 0.46; (2) 2.1; (3) 11.6; (4) 41.8 mils. The devices were photolithographically defined after irradiation.

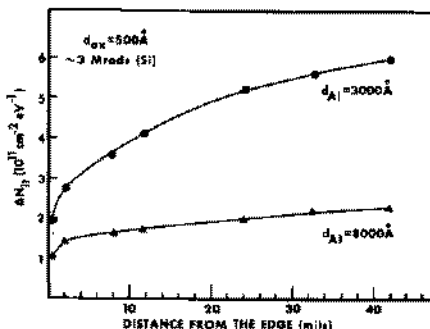


Fig. 10 Dependence of the radiation-induced interface trap peak density on the distance from the device edge for two Al thicknesses.

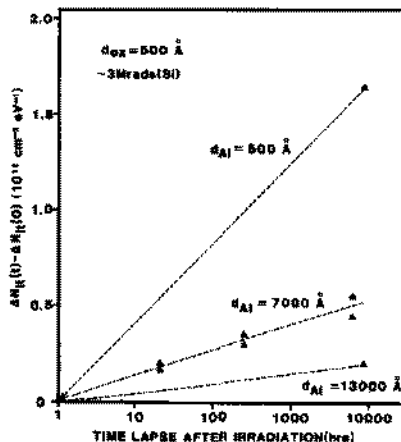


Fig. 11 Change in the radiation-induced interface trap peak density with time after the completion of the irradiation for three Al thicknesses.

DISCUSSION

The gate thickness dependence, stress relaxation effect, and edge effect experiments suggest that the interface trap generation by ionizing radiation is strongly affected by the stress distribution in the MOS structure. In previous publications [13,14] we mentioned two possible mechanisms that could explain our results. One of these involves the changes in the interfacial strained bonds induced by the gate Al. While the overall gate Al induced macroscopic interfacial strain in the samples under discussion appears to be relatively small, (in the range of 0.1 - 1%) it nevertheless could cause as many as 10^{12} - $10^{13}/\text{cm}^2$ (0.1% - 1% of $10^{15}/\text{cm}^2$) interfacial atomic bonds to undergo significant changes in bond length (on the order of a fraction of 1Å) or equivalent bond angle, provided that the strain is preferentially distributed among sites that are more susceptible to distortion under an external force. Such sites might correspond to those that are near a defect or an impurity center. During ionizing radiation, many of the atomic bonds are broken, resulting in generation of electron-hole pairs. Accompanying the bond breaking process is bond reformation, the probability of which depends on the relative positions of the ionized atoms and their local environments.

In a region where a high density of strained bonds exists, the breakage of bonds by ionizing radiation will be followed by relaxation of the ionized atoms to new equilibrium positions with a low probability of bond reformation, thus forming localized energy levels, as proposed by Gwyn [10]. It can be seen from Figs. 4 and 5 that 1) PMA treatment; (2) increasing the gate Al thickness; and 3) decreasing the time between PMA and irradiation all result in a more compressed silicon surface at the SiO_2 interface. The data of Fig. 7 therefore suggest that, in accordance with the model, the bond reformation process is more favorable with the Si surface under compression, resulting in less radiation induced traps with increasing compressive stress at the interface. The edge effect can also be explained with this model. Since the compressive stress at the silicon surface induced by the Al layer will be largest at the edge, it is expected that devices closer to the edge will have less radiation-induced interface traps.

Alternatively, the results can be explained by an oxide bond strain gradient model proposed by Grunthaler, et al. [5] In that model, the generation of interface traps can be the result of the propagation of radiation-induced defects in the strained region to the SiO_2/Si interface. The extent of this propagation depends on the oxide bond strain gradient such that small gradient values lead to less radiation damage.

To discuss the effect of the oxide bond strain gradient on the defect propagation process in SiO_2 , in Fig. 12 we illustrate qualitatively the strain distribution near the SiO_2/Si interface. The intrinsic oxide strain distribution [5] is represented by the thin solid curve. The gate Al induces an additional strain gradient, the direction of which is opposite to the intrinsic strain gradient (see Eq. 2). This is shown by the dotted lines for two different Al thicknesses. The resultants (1) and (2) (thick solid curves) are obtained by adding the intrinsic strain curve to the respective Al-gate induced curve.

Note that the gradient of the resultant (2) curve near the SiO_2/Si interface is smaller than that of resultant (1), which should lead to a smaller density of radiation-induced interface traps for the thick Al sample. In addition, both resultant curves exhibit a maximum (marked X_{m1} and X_{m2} , respectively), whose location moves closer to the SiO_2/Si interface as the gate Al gets thicker.

According to the oxide bond strain gradient model, the radiation induced defects tend to propagate in the direction of increasing bond strain. Therefore, it is not unreasonable to speculate that only those defects generated to the right of X_m would migrate to the SiO_2/Si interface and create interface traps. Since X_{m2} is closer to this interface than X_{m1} , the sample with thick Al would thus collect fewer such defects at the SiO_2/Si interface due to its smaller effective collection depth.

It is also imperative to mention that although in this example we use curves (1) and (2) in Fig. 12 to represent the effect of thin and thick Al gates, they could equally well be labeled as 'No PMA' and 'PMA', or 'A long time after PMA' and 'Immediately after PMA', or 'Far away from the edge' and 'Right at the edge', respectively. In other words, curves (1) and (2) are only representative of a pair of samples with different amounts of Al-induced oxide stress, which has been measured, and it is of no consequence how these curves are produced.

Since both models are equally consistent with our results, additional information is necessary to determine which mechanism may be dominating. The experimental data which shed some light with regard to this is shown in Fig. 11, where we display the growth of ΔN_{it} as a function of time lapse after the completion of the irradiation.

According to the Si-surface stress model, the density of radiation-induced traps should depend on the strained bonds which are present right at the interface during irradiation so that once the irradiation is terminated, the atoms quickly occupy their new equilibrium positions, and broken bonds are formed, causing interface traps. Therefore, one would expect to see either little change in ΔN_{it} after irradiation on the time scale shown in Fig. 11, or some slight annealing at room temperature.

On the other hand, in the oxide bond strain gradient model, a defect propagation mechanism through the strained region is involved, and the rate of propagation depends on the strain gradient.

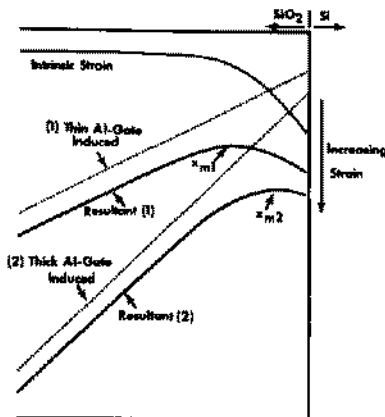


Fig. 12 Qualitative diagram illustrating the strain distribution in the oxide and the effect of the gate electrode on it.

This process could continue indefinitely until all the defects in the strained region are removed, and thus a time dependent growth of AN_{it} would be entirely reasonable. Referring back to Fig. 12, we see that the strain gradient near the SiO_2/Si interface is larger for the thin Al sample, which is therefore expected to exhibit a faster growth of AN_{it} with time than that of the thick Al sample. This is again consistent with the data shown in Fig. 11.

A crucial point in the evaluation of the oxide bond strain gradient is that it need not be considered independently from the hydrogen model. In fact, it has been suggested that the presence of water or hydrogen related sites can facilitate the defect propagation process [5], thereby increasing the density of radiation induced interface traps. Therefore, in order to study interfacial stress related effects, it is important to ensure that the samples have the same oxide quality, particularly in terms of their hydrogen and water contents. Conversely, the gate electrode parameters should be kept the same if one wants to investigate the effect of hydrogen. Failure to do so could lead to erroneous results and conclusions.

In summary, the interfacial stress distribution in a MOS structure can be significantly altered by the mechanical properties of the gate metal film, which in turn modulates the generation of interface traps resulting from ionizing radiation. Our experimental results are consistent with a model which incorporates the effect of this gate-induced stress distribution on the oxide bond strain gradient near the SiO_2/Si interface.

ACKNOWLEDGMENT

This work was supported by the Semiconductor Research Corporation under contract number 83-01-018, the Defense Nuclear Agency, and the Naval Research Laboratory under contract number N00014-83-0539.

REFERENCES

1. F.B. McLean, IEEE Trans. Nucl. Sci. NS-27, 1651 (1980).
2. C.M. Svensson in The Physics of SiO_2 and its Interfaces, ed. by S.T. Pantelides, (Pergamon, New York, 1978), p. 328.
3. M. Pepper, Thin Solid Films 14, 57 (1972).
4. C.T. Sah, IEEE Trans. Nucl. Sci. NS-23, 1563 (1976).
5. F.J. Grunthauer, P.J. Grunthauer, and J. Maserjian, IEEE Trans. Nucl. Sci. NS-29, 1462 (1982).
6. F.J. Grunthauer, B.F. Lewis, N. Zamini, and J. Maserjian, IEEE Trans. Nucl. Sci. NS-27, 1640 (1980).
7. H.L. Hughes, IEEE Trans. Nucl. Sci. NS-16, 195 (1969).
8. T-P. Ma, G. Scoggan, and R. Leone, Appl. Phys. Lett. 27, 61 (1975).
9. T-P. Ma, Appl. Phys. Lett. 27, 615 (1975).
10. C.W. Gwyn, J. Appl. Phys. 40, 4886 (1969).
11. M-R. Chin and T-P. Ma, Appl. Phys. Lett. 42, 883 (1983).
12. E.P. BerNisse, Appl. Phys. Lett. 30, 290 (1977).
13. V. Zakeriya and T-P. Ma, J. Appl. Phys. 56, 1017 (1984).
14. V. Zakeriya and T-P. Ma, Appl. Phys. Lett. 45, 249 (1984).
15. V. Zakeriya and T-P. Ma, Appl. Phys. Lett. 43, 95 (1983).
16. R.J. Jacobine and W.A. Schiegel, J. Appl. Phys. 37, 2429 (1968).
17. V. Zakeriya and T-P. Ma, unpublished.
18. W.A. Brantley, J. Appl. Phys. 44, 534 (1973).
19. Values for Fused Silica, CRC Handbook of Tables for Applied Engineering Science, 2nd ed., CRC Press.
20. J.H. Srebrinsky, Solid-State Electronics 13, 1455 (1970).
21. A. Bloch and E.S. Meieran, J. Appl. Phys. 38, 2913 (1967).
22. B.C. Wonsiewicz and D.V. McCaughan, J. Appl. Phys. 44, 5476 (1973).
23. P.S. Winokur, J.M. McGarrity, and H.E. Boesch, Jr., IEEE Trans. Nucl. Sci. NS-23, 1580 (1976).
24. P.S. Winokur, H.E. Boesch, Jr., J.M. McGarrity, and F.B. McLean, J. Appl. Phys. 50, 3492 (1979).